

Moving Out: Physically-grounded Human-AI Collaboration

Xuhui Kang Sung-Wook Lee Haolin Liu Yuyan Wang Yen-Ling Kuo

University of Virginia

{xuhui, dcs3zc, srs8rh, ntc8tt, ylkuo}@virginia.edu

Abstract

The ability to adapt to physical actions and constraints in an environment is crucial for embodied agents (e.g., robots) to effectively collaborate with humans. Such physically grounded human-AI collaboration must account for the increased complexity of the continuous state-action space and constrained dynamics caused by physical constraints. In this paper, we introduce *Moving Out*, a new human-AI collaboration benchmark that resembles a wide range of collaboration modes affected by physical attributes and constraints, such as moving heavy items together and maintaining consistent actions to move a big item around a corner. Using *Moving Out*, we designed two tasks and collected human-human interaction data to evaluate models' abilities to adapt to diverse human behaviors and unseen physical attributes. To address the challenges in physical environments, we propose a novel method, BASS (Behavior Augmentation, Simulation, and Selection), to enhance the diversity of agents and their understanding of the outcome of actions. Our experiments show that BASS outperforms state-of-the-art models in AI-AI and human-AI collaboration. The project page is available at https://live-robotics-uva.github.io/movingout_ai/.

1 Introduction

Humans can quickly adapt their actions to physical attributes (e.g., sizes, shapes, weights, etc.) or physical constraints (e.g., moving with stronger forces, navigating narrow paths, etc) when collaborating with other agents in the physical world. This ability is critical when embodied agents (e.g., robots) need to collaborate with humans to complete real-world tasks, such as assembly, transporting items [1–5], cooking [6], and cleaning [7, 8]. In these scenarios, successful interactions require understanding physical attributes and constraints while aligning with human behavior.

Prior work [6, 9, 10, 8, 11, 12] has explored human-AI collaboration in discrete space or task level, which often has simplified interaction dynamics compared to the real world. As shown in Fig. 1, physically grounded tasks have increased the diversity of physical constraints, physical variations, and human behavior. While physical constraints, such as narrow passages, restrict movement and require precise coordination, there are still a large number of rotations and ways of holding objects that can lead to successful collaborations. In this paper, we propose *Moving Out*, a novel benchmark inspired by the *Moving Out* game [13], to address dynamic physical interactions and diverse collaboration scenarios in a physically grounded setting.

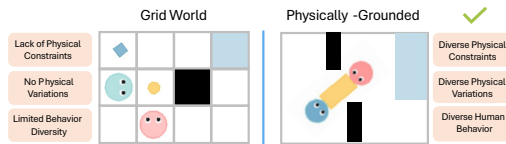


Figure 1: Multiagent collaboration in a grid world vs. in a physically-grounded setting. Physically grounded settings introduce diverse physical constraints, attributes, and actions which increase the complexity when an AI agent needs to collaborate with humans.

While AI-AI collaboration can achieve strong collaborative performance through methods like self-play [14], the resulting AI agents often struggle to adapt to human-AI collaboration, where human partners exhibit diverse and unpredictable behaviors [15]. This is particularly pronounced in physically grounded settings where minor variations in human actions, such as lifting angles or applying force, can significantly affect outcomes. An agent needs to understand the physical consequences of actions to generalize behavior across different scenarios.

We design two tasks to evaluate an agent’s ability to adapt to diverse human behavior and to understand physical constraints. The first requires the agent to play against an trained with diverse human behavior. We collected over 1,000 pairs of human demonstrations on maps with fixed physical properties from 36 human participants. These demonstrations capture a wide range of behaviors for identical set of tasks. The second requires the agent to generalize to unseen physical attributes and constraints. We collected 700 pairs of expert demonstrations (from 4 experts) on maps with randomized object properties, such as mass, size, and shape. Together, these tasks provide a framework for testing the adaptability and generalization of embodied agents in diverse, physically grounded settings.

To further address the challenges of the continuous state-action space and constrained transitions in physical environments, we propose a novel approach, BASS (Behavior Augmentation, Simulation, and Selection), which significantly outperforms prior works. First, we augment the dataset by enhancing the diversity of the agent’s collaborative partners. When an agent’s start and end poses in one sub-trajectory match the sub-trajectory in another interaction, we can swap the partner’s states to create new trajectories. This enables the agent to generate consistent behavior when the partner’s behavior has small variations. Second, we train a dynamics model of the interaction so we can simulate the outcome of an action for a given state. We use this predicted state to score action candidates, allowing the agent to select actions that are more effective given the physical constraints.

We evaluate BASS on the two proposed tasks in AI-AI and human-AI collaboration settings. We show that BASS outperforms baselines across key metrics such as task completion and waiting time. We also conducted a user study to evaluate the model’s performance against human participants, demonstrating the effectiveness of BASS in coordinating and assisting real humans.

In summary, our work makes the following contributions: (1) We introduce *Moving Out*, an environment for physically grounded human-AI collaboration. (2) We propose two tasks to examine how human behavior and physical constraints impact collaboration and collect a dedicated human dataset for model training and evaluation. (3) We develop *Behavior Augmentation, Simulation, and Selection* (BASS), which significantly improves human-AI collaborative performance.

2 Related Work

Environments for Human-AI Collaboration Several multi-agent environments [16, 17] have been proposed for multi-agent reinforcement learning (MARL). Many of them are competitive rather than cooperative. For studying human-AI collaboration, existing environments have focused on different aspects. OvercookedAI [6], LBF [11], and RWARE [11] are discrete environments where agents coordinate to pick and place items, but they have limited physical attributes and constraints. The discrete state-action space also limits the diversity of agent behaviors. It Takes Two [9] involves two agents carrying a table together, but since the agents are bound to the table and cannot move freely, it does not capture scenarios requiring independent task division, collision avoidance, or awareness of when help is needed. HumanTHOR [7] and Habitat 3.0 [8] provide realistic simulation, but the collaboration in these simulators are task level or coordination in navigation. Watch and Help [18] evaluates human-AI collaboration from a social perception perspective, overlapping with our awareness collaboration mode. But their agent collaboration only considers task division and does not include physical attributes. Other studies [19, 20] also explored human-AI collaboration using the Hanabi game [21], but Hanabi is based on sequential cooperation rather than simultaneous embodied teamwork. Moving Out provides diverse collaboration modes and focuses on how AI can learn to collaborate with humans to improve task performance in continuous environments with diverse physical attributes, constraints, and human behavior. For a summarized comparison, see Appx. A.

Learning Human-AI Collaboration Policy Behavior Cloning (BC) learns human-AI collaboration policies from expert data, commonly using models like MLP [22], GRU [23], or diffusion policies [24]. Building upon BC, several studies have explored simulation and action selection methods relevant to our approach in various contexts. For instance, Wang et al. [25] utilized future state prediction for scoring actions in autonomous driving. In multi-agent scenarios, Yuan et al. [26] proposed

AgentFormer for forecasting interactive agent behaviors. Concurrently, Ding et al. [27] investigated the use of world models to predict future states based on internal knowledge. Furthermore, q-VAE [28] applies latent space transformations for next-state prediction, and Zhao et al. [29] introduced a trajectory prediction method that scores entire future trajectories to inform decision-making. Additionally, some approaches leverage RL to train collaborative agents. Building upon self-play [14] and population-based training, several works [15, 30–36] enhance agents’ ability to achieve zero-shot coordination by encouraging behavioral diversity during training and exploration. In addition, multi-agent RL algorithms, like MAPPO [37] and MADDPG [38], can also be employed to train agents for potential human-AI collaboration. However, these approaches train only through self-play and do not use human data. Some studies [39, 15] further align policies with human behavior by integrating BC models trained with human data into self-play, so that human data stays in the RL learning loop.

Evaluating Human-AI Collaboration Research on human-AI collaboration has focused on evaluating and improving AI agents across different settings. Some works redefine evaluation criteria beyond task performance, incorporating aspects like trust and perceived cooperativity [20]. In AI-assisted decision-making scenarios, prior work [40] directly computes the accuracy of AI decisions. Some works [41, 31, 36] focus on training RL agents to adapt to diverse partners and evaluate the agents by the score when playing with humans. Similarly, LLM-based agents [42] are evaluated by final score and time efficiency. Several works [36, 20, 19, 43, 44] design questionnaires to evaluate different aspects like human-like, trustworthiness, fluency, and warmth.

3 Problem Definition

We model human-AI collaboration as a decentralized Markov decision process (Dec-MDP) [45, 46], defined as a tuple $\mathcal{M} = (\mathcal{S}, \mathcal{A}, \mathcal{P}, r, \mathcal{O}, \gamma, T)$, where \mathcal{S} is the joint state space, and $\mathcal{A} = \mathcal{A}^i \times \mathcal{A}^j$ is the joint action space of the two agents. The transition function $\mathcal{P} : \mathcal{S} \times \mathcal{A} \times \mathcal{S} \rightarrow [0, 1]$ is the probability of getting the next state given a current state and a joint action. The reward function $r : \mathcal{S} \times \mathcal{A} \rightarrow \mathbb{R}$ specifies the reward received for each state-joint-action pair. The observation function $\mathcal{O} : \mathcal{S} \rightarrow \mathcal{O}^i \times \mathcal{O}^j$ generates an observation for each agent for a given state. The observation of each agent makes the state jointly fully observable. The discount factor $\gamma \in [0, 1]$ determines the importance of future rewards, and T is the time horizon of the task.

At each timestep t , the environment is in a state $s_t \in \mathcal{S}$. Agents π^i observes $o_t^i \in \mathcal{O}$, where \mathcal{O} is the observation space derived from s_t , and selects an action $a_t^i \in \mathcal{A}^i$ according to its policy $\pi^i : \mathcal{O} \rightarrow \mathcal{A}^i$. The joint action $a_t = (a_t^i, a_t^j)$ transitions the environment deterministically to a new state $s_{t+1} \sim \mathcal{P}(\cdot | s_t, a_t)$. The trajectory of an episode is defined as $\tau = (s_0, a_0, s_1, \dots, s_{T-1}, a_{T-1}, s_T)$, and the discounted return for the trajectory is: $R(\tau) = \sum_{t=0}^{T-1} \gamma^t r(s_t, a_t)$. The objective of each agent is to maximize the expected return $J(\pi^i, \pi^j) = \sum_{\tau} R(\tau)$ where the return is evaluated over the trajectories induced by the policies (π^i, π^j) .

Challenges when Collaborating with Humans When one of the agents is a human, the human agent may have diverse behaviors [6]. The AI agent must adapt its policy π^i to a wide range of potential human policies π^j . At inference time, we assume that the real human policy π^j is drawn from a universal but unknown human policy distribution \mathcal{D} . Thus, the AI agent’s optimal policy is:

$$\pi_{\star}^i = \arg \max_{\pi^i} \mathbb{E}_{\pi^j \sim \mathcal{D}} \mathbb{E}_{\tau \sim (\pi^i, \pi^j)} [R(\tau)]$$

where $\mathbb{E}_{\tau \sim (\pi^i, \pi^j)}$ denotes the expectation over τ where the actions are drawn from π^i and π^j respectively. Since the ground-truth distribution \mathcal{D} is unknown, the AI must use limited data to generalize across diverse human strategies.

The physical embodiment of agents and the physical environment introduce significant challenges for this human-AI collaboration framework. First, the continuous variables, such as positions and directions, increase the number of configurations in the state space. For example, there are multiple configurations that the agents can take to rotate an object together. The AI agent must optimize its policy under diverse human behaviors while ensuring robustness across a continuous and high-dimensional state space. Second, the state space \mathcal{S} also includes continuous physical variables such as object positions, orientations, and attributes (e.g., shape, size, and mass), which can create several constraints to limit the feasible state transitions \mathcal{P} . For instance, when two agents jointly move an object, the physical properties of an object (e.g., its mass or shape) can influence the actions required

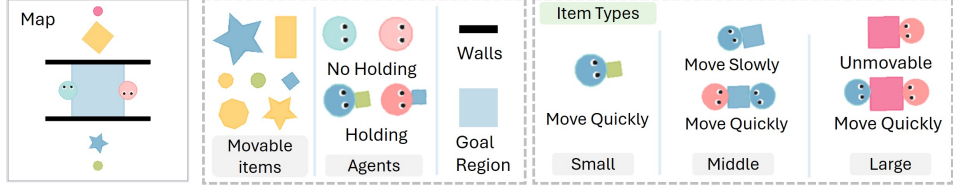


Figure 2: The *Moving Out* environment requires two agents to collaboratively move objects to the blue goal region. The environment includes movable objects with varying shapes and sizes. An agent can move a small item quickly. As the object sizes increase, the agent needs the other’s help to move the object.

to achieve successful transitions. Objects with irregular shapes require agents to coordinate their grips at specific parts. Heavier objects demand synchronized application of two agent’s forces. Considering the physical constraints $\Gamma(s_t, a_t)$ that apply to the current state-action pair, the transition function is constrained as follows:

$$\mathcal{P}(s_{t+1} | s_t, a_t) = \begin{cases} 1, & \text{if } \Gamma(s_t, a_t) \text{ satisfies (transition to } s_{t+1}) \\ 0, & \text{if } \Gamma(s_t, a_t) \text{ does not satisfy (remains in } s_t) \end{cases}$$

These constraints create several narrow transitions, similar to prior studies about motion planning [47–49], and can further affect the agents’ collaboration strategies. For example, in scenarios where the agents need to move a rectangular sofa through a narrow doorway, the agents need to grasp the shorter sides of the sofa to move and coordinate their moves to ensure they can fit through the entrance without collision. In this paper, we study human-AI collaboration under the challenges of continuous state space and constrained transitions introduced by physical embodiments and environments.

4 Moving Out Environment and Dataset

4.1 Environment

To test how physical environments can affect human-AI collaboration, we need an environment that follows physics. We build *Moving Out* on top of a single-agent environment *Magical* [50, 51] where agents and objects are physical bodies moving in a 2D physics simulation. As shown in Fig. 2, each agent can maneuver freely in *Moving Out* and can move objects with varying degrees of difficulty depending on the object size and shape. The goal is to transport all objects to the goal regions. This design emphasizes flexibility, allowing agents to act independently while also creating scenarios where collaboration is necessary for efficient task completion.

4.1.1 Physical Variables

The environment includes these physical components: movable items, walls, and goal regions.

Movable Items are controlled by the following variables to introduce diverse physical interactions.

- **Shapes** include stars, polygons, and circles, each requiring unique grabbing and rotation strategies.
- **Sizes** include small, medium, and large, each has increasing difficulty in moving, and can slow the speed of an agent.
- **Mass** are varied for different items. This influences an agent’s moving speed during transportation.

Walls introduce friction. Agents that collide with walls experience reduced moving speed, adding another layer of complexity.

Goal regions are designated areas larger than the total size of items. Agents must carefully arrange items to ensure all items can fit in the region, requiring precise spatial planning and coordination.

4.1.2 Layout Types

The physical variables introduce diverse collaborative behavior in *Moving Out* as illustrated in Fig. 3. A successful collaboration usually requires a mixture of different behaviors. Specifically, we designed

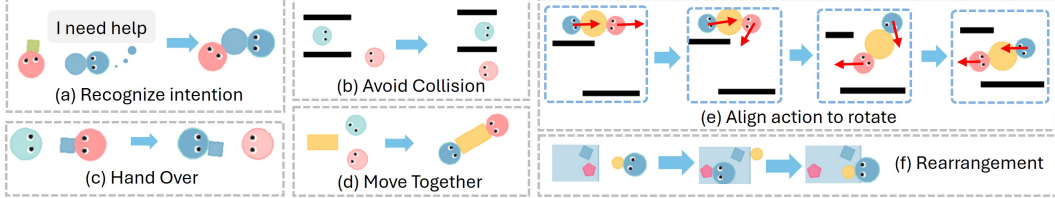


Figure 3: Diverse collaboration behaviors in *Moving Out*, including (a) recognizing when help is needed, (b) avoiding collisions, (c) passing objects, (d) moving items together, (e) aligning actions, and (f) organizing objects in the goal region.

12 maps that focus on three collaboration modes. See example maps in Fig. 4 and Appx. L for the full set of maps.

Coordination The maps in this category only include small items, so each agent can complete the task independently. However, we add narrow passages in the maps. These passages often block an agent’s route, requiring the other to move aside or pass the item. For example, in Map 1 (Hand Off), the blue agent must pick up the item and, because of the narrow passage, pass it to the pink agent. This setup enforces cooperation, as the task cannot be completed without coordination between the two agents.

Awareness The maps in this category do not have a clear optimal sequence for moving items, requiring agents to decide whether, when, and how to assist their partner for efficiency. For instance, in Map 6 (Distance Priority), each agent starts near multiple items and must decide whether to handle nearby items first, assist their partner, or prioritize tasks independently. These decisions become even more complex when collaborating with a human partner, as human behavior can vary significantly. A human partner might wait for AI help with larger items, adopt a passive approach, or focus on smaller tasks independently. This variability demands that the AI agent dynamically adapts to the human’s behavior.

Action Consistency This scenario requires agents to maintain consistent and synchronized actions over time, such as continuously aligning their efforts to move and rotate large items together. The challenge is aligning force directions and dynamically adjusting them to ensure efficient movement while navigating around tight spaces or obstacles. For instance, in Map 12 (Sequential Rotations), two agents must collaboratively transport a large item through a series of narrow passages. Throughout this process, the agents must continually synchronize their actions to rotate and adjust the item’s angle, allowing it to fit through the openings. Misalignment in their efforts could result in the item becoming stuck or unnecessary movements that waste time and energy.

4.2 Tasks

We design two tasks that evaluate a model’s ability to adapt to diverse human behaviors and to generalize to unseen physical attributes.

Task 1: Adapting to Diverse Human Behaviors in Continuous Environment The first challenge of physically grounded human-AI interaction arises from the continuous state-action space, which allows for a wide range of possible human behavior. To test whether an agent can adapt to diverse human behavior, we fixed the configurations of the 12 maps and collected the human-human collaboration data that demonstrate different ways to collaborate in the same maps. These demonstrations represent a finite set of human behaviors. In this task, we train a model on this dataset and evaluate it by testing it with different human or AI collaborators. This setup assesses whether the model can generalize beyond the observed behaviors to adapt to diverse human behavior. For an agent designed to assist humans effectively, learning to adapt from limited human demonstrations is crucial.

Task 2: Generalizing to Unseen Physical Constraints The second challenge arises from the physical constraints, which limit the possible transitions of given states. To test whether the agent

understands physical constraints, we randomized the physical attributes of objects in the 12 maps to collect human-human interaction data that demonstrates how humans adapt to changes in physical variables. Again, we train a model with the collected dataset and evaluate it on maps with unseen object attributes. To ensure the model learns the effects of physical constraints rather than memorizing them, we avoid having identical objects in the training and testing datasets. This forces the model to generalize and understand the impact of shape and type across varying physical configurations.

4.3 Dataset

The data collection was approved by the Institutional Review Board (IRB). Two human players control the agents with joysticks. The game ran at 10Hz, and on average, each map took around 30 seconds (or 300 time steps) to complete the transportation of all items. See Appx. H for details.

For Task 1, we recruited 36 college students as participants and collected over 1,000 human-human demonstrations (2,000 action sequences in total) across 12 maps. This ensures that the dataset captures a wide range of human behaviors, providing sufficient diversity for training and testing the model’s ability to generalize to unseen human strategies.

For Task 2, we emphasize the randomized properties of objects rather than the variable behaviors. In this case, we used 4 expert players to collect 720 human-human demonstrations (1,440 action sequences in total), with 60 demonstrations per map. Each map included randomized physical attributes, allowing us to evaluate the model’s ability to generalize to unseen object attributes.

5 BASS: Behavior Augmentation, Simulation, and Selection

To address the proposed tasks, we develop BASS (Behavior Augmentation, Simulation, and Selection) which considers the increased number of configurations in continuous space and the outcome of actions in physical environments. First, at training time, we augment the behavior data. This helps the model adapt to different behaviors better by exposing it to a broader range of possible interactions. Second, we train a dynamics model to simulate the outcome of an action. At inference time, the model can select actions by evaluating the predicted states. This enables the model to handle uncertainty from physical constraints and adapt its decisions accordingly.

5.1 Collaboration Behavior Augmentation

Our augmentation strategy involves two techniques:

Generating New States by Perturbing the Partner’s Pose For a given trajectory, we generate new states by introducing noise to the partner’s pose while keeping all other state variables unchanged. This perturbation creates additional observation variations in training data, allowing the agent to experience a broader range of possible partner behaviors. Since human actions naturally vary, this approach helps improve the agent’s robustness to small deviations in the partner’s movements while maintaining its own task objectives. This perturbation is expressed as $\tilde{p}_{\text{partner}} = p_{\text{partner}} + \epsilon$, $\epsilon \sim \mathcal{N}(0, \sigma^2)$ where p_{partner} is the original partner’s pose, ϵ is Gaussian noise with mean 0 and variance σ^2 , and $\tilde{p}_{\text{partner}}$ is the perturbed pose used to generate new state variations.

Recombination of Sub-Trajectories Each global state s_t can be decomposed into $s_t = (s_t^i, s_t^j, s_t^e)$, where s_t^i and s_t^j are the individual states of agent i and j , and s_t^e captures the remaining environment-specific information. Given a trajectory $\tau = \{(s_t, a_t)\}_{t=1:T}$, we extract three sequences: $\tau^i = \{(s_t^i, a_t^i)\}_{t=1:T}$ is the state-action sequence of agent i ; similarly τ^j is the state-action sequence of agent j and τ^e is the sequence of environment information. We have $\tau = \tau^i \cup \tau^j \cup \tau^e$. Moreover, let $\tau_t^i = (s_t^i, a_t^i)$ be the t -th state-action pair of agent i , and define $\tau_{t_1:t_2}^i = (s_{t_1}^i, a_{t_1}^i, \dots, s_{t_2}^i, a_{t_2}^i)$ as the continuous sub-trajectory of τ^i from t_1 to t_2 . We can define i ’s trajectory composed of sub-trajectories $\tau^i = \tau_{1:t_1-1}^i \cup \tau_{t_1:t_2}^i \cup \tau_{t_2+1:T}^i$; and similarly for j .

Given τ and two time step t_1, t_2 , we can search for another trajectory $\hat{\tau}$ in the dataset such that $\hat{\tau}_{t_1}^i = \tau_{t_1}^i$ and $\hat{\tau}_{t_2}^i = \tau_{t_2}^i$. We can then construct two new trajectories by swapping agent j ’s subsequences between t_1 and t_2 :

$$\tau^i \cup \left(\tau_{1:t_1-1}^j \cup \hat{\tau}_{t_1:t_2}^j \cup \tau_{t_2+1:T}^j \right) \cup \tau^e \quad \text{and} \quad \hat{\tau}^i \cup \left(\hat{\tau}_{1:t_1-1}^j \cup \tau_{t_1:t_2}^j \cup \hat{\tau}_{t_2+1:T}^j \right) \cup \tau^e$$

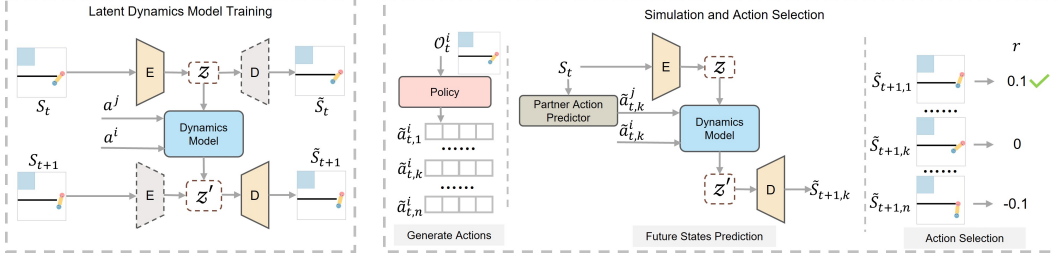


Figure 5: Overview of our Simulation and Action Selection components. **(Left)** The latent dynamics model that encodes the latent state from t to $t + 1$ to enable next state prediction. **(Right)** The action selection pipeline: The policy first generates candidate actions. The dynamics model then estimates the resulting future states, and finally, the best action is selected based on state evaluation.

By aligning the start and end of agent i 's sub-trajectory, the generated trajectories maintain temporal consistency for agent i while introducing a different partner sequence. This approach enriches the training set with new, valid trajectories where agent i 's behavior is fixed and the partner's varies.

Validity of the Generated States We can validate generated sub-trajectories based on the state information. Specifically, one can check whether the generated states remain within the valid state space and do not result in conflicts, such as collisions or other inconsistencies. However, we will show in the experiment section that, even without explicit validation, this augmentation strategy can improve performance.

5.2 Simulation and Action Selection

To understand the outcome of an action, in simulation environments, we can utilize the physics engine to simulate the action outcome. However, in real-world settings where a simulator is unavailable, a world model or next state predictor is required. Fig. 5 shows the training and inference pipelines of our Simulation and Action Selection components.

Next State Prediction Our next state predictor utilizes two autoencoders to estimate future states. First, one autoencoder encodes the current state into the latent space. The dynamics model then takes this latent representation along with the actions of both agents as input to predict the latent representation of the next state. Finally, this predicted latent representation is decoded by another autoencoder to reconstruct the next state. Since the next state depends on the agent's own action and the partner's action, we use a partner action predictor to estimate the partner's action based on the current state. Practically, the partner's predictor can share the same architecture as the agent's policy or directly use the agent's own policy by swapping its state with the partner's state to predict the partner's action. The dynamics model predicts the future state as: $z_{t+1} = f(z_t, a_t, a_t^{(p)})$, where z_t and z_{t+1} represent the latent spaces of the current and future states, a_t is the agent's action, $a_t^{(p)}$ is the inferred partner's action, and f is the dynamics model.

Action Selection Once the next state is predicted, the reward for each action is computed based on the total distance of all objects to the goal region. We use Normalized Final Distance (NFD) as defined in Sec. 6, but other metrics that measure partial progress of map completion also suffice. We then select the action with the highest reward as the optimal action: $a^* = \arg \max_{a_i} r(a_i), i = 1, 2, \dots, n$, where $r(a_i)$ is the reward for action a_i . This approach enables the model to choose the most effective action, even in real-world scenarios without access to a simulator.

6 Experiment

We aim to answer the following research questions: **(RQ1)** How well do existing methods and BASS perform in physically grounded settings? **(RQ2)** Does BASS better support humans and work more effectively with them in physically grounded collaboration? **(RQ3)** What are the limitations of existing methods and BASS in physically grounded human-AI collaboration?

To answer these questions, we train and test all methods on the two Moving Out tasks to compare their performance. First, each model plays with itself. This demonstrates each model's ability to handle

physical constraints in a controlled setting (i.e., without the variability introduced by actual humans). Then, we let each model play with humans to evaluate their interactions with diverse behaviors.

6.1 Settings

Baselines We compare BASS against these behavior cloning and RL baselines to predict actions:

- **MLP** is a common behavior cloning baseline.
- **GRU** captures temporal dependencies of state and actions using recurrent connections.
- **Diffusion Policy (DP)** [24] captures multimodal distribution and has demonstrated strong performance across various tasks.
- **MAPPO** [37] is a commonly used multi-agent RL algorithm. It has demonstrated strong performance in cooperative games. See Appx. C for details about training and reward settings.

Evaluation Metrics We measure the success of collaboration using the following metrics: (1) Task Completion Rate (TCR) for size-weighted successful item delivery; (2) Normalized Final Distance (NFD) for the distances between objects and the target, measuring partial progress; (3) Waiting Time (WT) for the amount of time an agent waits for assistance with large items; and 4) Action Consistency (AC) for the degree of force alignment when moving items jointly, indicating coordination efficiency. Detailed definitions are in Appx. F.

Human Subject Study Our study was approved by the IRB. We conducted a human subject study with 32 participants to evaluate BASS against the DP baseline in both tasks. Each participant played 32 maps in total, cooperating with each method in two rounds per map. After completing the first round, the participant and model switched to control the other agent. Upon finishing all maps, participants were given a questionnaire to capture subjective feedback. See Appx. J for details.

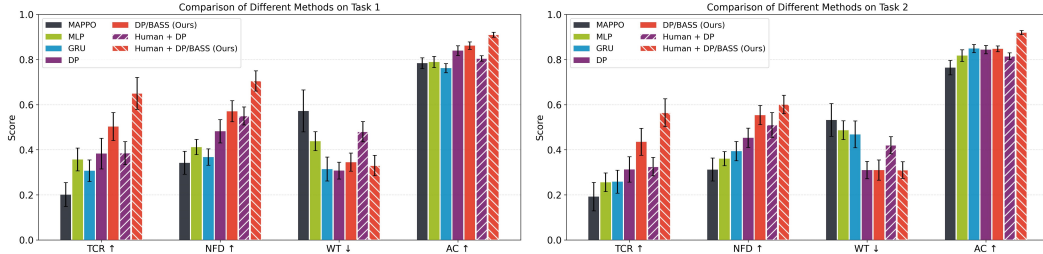


Figure 6: BASS outperforms baselines on Task 1 and Task 2, against AI (solid) and humans (striped).

6.2 Results

Collaboration with AI Itself (RQ1) Fig. 6 compares BASS with baselines in Task 1 and Task 2 by running 20 times on each map with different random seeds. BASS outperforms baselines, especially in task completion metrics TCR and NFD. For WT, DP performs better than GRU, MLP, and MAPPO, implying that it more promptly assists the other agent whenever help is needed. In terms of action consistency, there is no significant gap among methods; a potential reason is that each model is paired with itself and thus pursues the same objectives. Overall, the RL agents exhibit behaviors that follow the dense reward setting, while the BC agents mainly reflect behaviors present in the dataset. A detailed comparison of the behaviors between BC and RL agents can be found in the Appx. E.

In task 1, DP outperforms baselines in TCR and NDF, suggesting that DP effectively learns cooperative behaviors. MLP shows the longest waiting times, implying that it often leaves one agent waiting for help. By contrast, BASS reduces waiting time, likely because the scoring mechanism prioritizes overall task progress. In task 2, BASS shows stronger performance, likely because it evaluates the impact of each action on the generated state, leading to a better grasp of how to help when dealing with objects that exhibit different physical properties.

Collaboration with Humans (RQ2) The bars with stripes in Fig. 6 show the results with humans. In both tasks, BASS significantly improved task completion rates (TCR and NFD) compared to the DP. This indicates that BASS adapts better to human behavior. For wait time, DP increased when playing with humans, suggesting it struggles with different humans, despite that DP captures multimodal distributions. BASS reduced wait time, demonstrating its ability to adapt to diverse human behaviors. For action consistency, DP performed worse because it cannot handle differences between the evaluation and training data. BASS used diverse collaborative behaviors during training and selected the best actions for interacting with humans, resulting in better consistency.

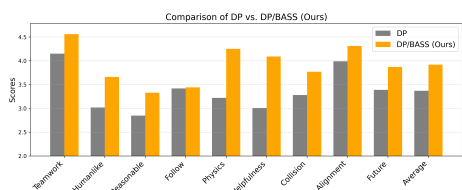


Figure 7: User survey results in a 7-point Likert scale

Methods	Task 1		Task 2	
	TCR↑	NFD↑	TCR↑	NFD↑
GRU	0.3070	0.3674	0.2582	0.3935
+ BASS w/o Simulation	0.4117	0.4396	0.3333	0.4141
+ BASS w/o Augmentation	0.3531	0.4047	0.3670	0.4246
+ Full BASS	0.4120	0.4454	0.3414	0.4410
Diffusion Policy (DP)	0.3829	0.4818	0.3125	0.4526
+ BASS w/o Simulation	0.4028	0.5114	0.3569	0.4908
+ BASS w/o Augmentation	0.4741	0.5561	0.4200	0.5187
+ Full BASS	0.5027	0.5707	0.4348	0.5535

Table 1: Ablations showing the impact of each component, we show BASS with GRU and DP backbones.

Human Feedback (RQ2) Fig. 7 summarizes post-experiment survey results from humans. We compare BASS with DP. The results show that BASS significantly outperformed DP in the Helpfulness category, indicating that BASS is better at consciously assisting others. Additionally, BASS demonstrated a better understanding of physics, suggesting that our next state predictor effectively comprehends and evaluates different actions to choose the best ones. Independent t-tests revealed that these differences are statistically significant ($p = 0.017$).

Ablations Table 1 shows the ablation of each component. Adding augmentation and simulation components improves task completion TCR and NFD compared to their base models. When using all components (full BASS), they achieve the highest overall performance in most cases.

Failure case study (RQ3) Fig. 8 shows examples of common failure cases from DP. In task 1, as illustrated in failure case 1, many participants reported that the AI agent frequently holds an item without passing it, resulting in frequent collisions. Additionally, participants noted that the AI agent often failed to come to assist, as shown in failure case 2, where a human agent (blue) was slowly pulling an item, but the AI agent (pink) instead went to grasp other smaller objects. These issues show the model’s limited ability to adapt to diverse behaviors, making it difficult to respond appropriately to actions that were not present in the training dataset. In task 2, most participants pointed out failure case 3, where the AI agent reached the target item but was unable to successfully grasp it. This indicates that the model struggles when encountering objects that were not in the training data. In contrast, BASS shows fewer reported failure cases than DP. Manual inspection revealed that BASS reduced the occurrence rates of the three failure types from $\{0.797, 0.688, 0.906\}$ in DP to $\{0.343, 0.563, 0.484\}$. However, effectively addressing these failures remains a substantial challenge for future research.

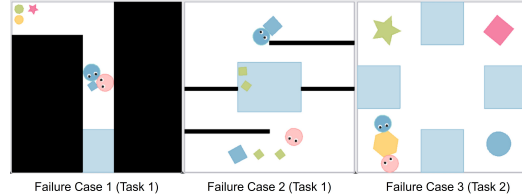


Figure 8: Failure case study: 1) Failing to release items during handover, 2) Not responding when assistance is needed, and 3) Inability to grasp large items upon approach.

where the AI agent reached the target item but was unable to successfully grasp it. This indicates that the model struggles when encountering objects that were not in the training data. In contrast, BASS shows fewer reported failure cases than DP. Manual inspection revealed that BASS reduced the occurrence rates of the three failure types from $\{0.797, 0.688, 0.906\}$ in DP to $\{0.343, 0.563, 0.484\}$. However, effectively addressing these failures remains a substantial challenge for future research.

7 Conclusion

We introduce *Moving Out*, a physically grounded human-AI collaboration benchmark that features a continuous state-action space and dynamic object interactions in a 2D physical environment. We created two challenging tasks and collected human-human collaboration data to enable future model development. Our evaluation results show that much remains to be done with existing models to effectively collaborate with humans in physical environments. Our proposed method, BASS, takes the first step to improve models’ adaptability to diverse human behaviors and physical constraints.

Limitations and Future Work While we conduct user studies using models, achieving smooth human-AI collaboration with generative models (e.g., DP, LLMs) remains challenging because of low inference speed. In our study, it requires at least 5~10Hz to have a smooth interaction (see Appx. I.2.) *Moving Out* aims to include diverse physical variations and collaboration modes; however, we do not cover all possible physical interactions. Future work includes improving generative models’ inference speed to achieve smooth human-AI collaboration in physical environments, leveraging LLMs’ reasoning abilities in physically grounded collaboration tasks, and extending to more complex cooperation dynamics among multiple AI agents and humans.

8 Acknowledgment

This work was supported by Toyota Research Institute and NSF CMMI-2443076. We acknowledge Research Computing at the University of Virginia for providing the computational resources and technical support that made the results in this work possible.

References

- [1] Francesco Semeraro, Alexander Griffiths, and Angelo Cangelosi. Human–robot collaboration and machine learning: A systematic review of recent research. *Robotics and Computer-Integrated Manufacturing*, 79:102432, 2023. ISSN 0736-5845. doi: <https://doi.org/10.1016/j.rcim.2022.102432>.
- [2] Thibaut Munzer, Marc Toussaint, and Manuel Lopes. Efficient behavior learning in human–robot collaboration. *Autonomous Robots*, 42:1103–1115, 2018.
- [3] Elena Corina Grigore, Alessandro Roncone, Olivier Mangin, and Brian Scassellati. Preference-based assistance prediction for human-robot collaboration tasks. In *2018 IEEE/RSJ International Conference on Intelligent Robots and Systems (IROS)*, pages 4441–4448. IEEE, 2018.
- [4] Sharath Chandra Akkaladevi, Matthias Plasch, Andreas Pichler, and Markus Ikeda. Towards reinforcement based learning of an assembly process for human robot collaboration. *Procedia Manufacturing*, 38:1491–1498, 2019.
- [5] Mirza Awais Ahmad, Mouloud Ourak, Caspar Gruijthuijsen, Jan Deprest, Tom Vercauteren, and Emmanuel Vander Poorten. Deep learning-based monocular placental pose estimation: towards collaborative robotics in fetoscopy. *International Journal of Computer Assisted Radiology and Surgery*, 15:1561–1571, 2020.
- [6] Micah Carroll, Rohin Shah, Mark K. Ho, Thomas L. Griffiths, Sanjit A. Seshia, Pieter Abbeel, and Anca Dragan. On the utility of learning about humans for human-ai coordination, 2020.
- [7] Chenxu Wang, Boyuan Du, Jiaxin Xu, Peiyan Li, Di Guo, and Huaping Liu. Demonstrating humanthor: A simulation platform and benchmark for human-robot collaboration in a shared workspace, 2024.
- [8] Xavier Puig, Eric Undersander, Andrew Szot, Mikael Dallaire Cote, Tsung-Yen Yang, Ruslan Partsey, Ruta Desai, Alexander William Clegg, Michal Hlavac, So Yeon Min, et al. Habitat 3.0: A co-habitat for humans, avatars and robots. *arXiv preprint arXiv:2310.13724*, 2023.
- [9] Eley Ng, Ziang Liu, and Monroe Kennedy III. It takes two: Learning to plan for human-robot cooperative carrying. *arXiv preprint arXiv:2209.12890*, 2022.
- [10] Georgios Papoudakis, Filippos Christianos, Lukas Schäfer, and Stefano V. Albrecht. Benchmarking multi-agent deep reinforcement learning algorithms in cooperative tasks, 2021.
- [11] Filippos Christianos, Lukas Schäfer, and Stefano Albrecht. Shared experience actor-critic for multi-agent reinforcement learning. *Advances in neural information processing systems*, 33:10707–10717, 2020.
- [12] Weihua Du, Qiushi Lyu, Jiaming Shan, Zhenting Qi, Hongxin Zhang, Sunli Chen, Andi Peng, Tianmin Shu, Kwonjoon Lee, Behzad Dariush, et al. Constrained human-ai cooperation: An inclusive embodied social intelligence challenge. In *The Thirty-eighth Conference on Neural Information Processing Systems Datasets and Benchmarks Track*.
- [13] Devm Games SMG Studio. https://store.steampowered.com/app/996770/Moving_Out/, 2020.
- [14] Gerald Tesauro. Td-gammon, a self-teaching backgammon program, achieves master-level play. *Neural computation*, 6(2):215–219, 1994.
- [15] Micah Carroll, Rohin Shah, Mark K Ho, Tom Griffiths, Sanjit Seshia, Pieter Abbeel, and Anca Dragan. On the utility of learning about humans for human-ai coordination. *Advances in neural information processing systems*, 32, 2019.

[16] Joel Z. Leibo, Edgar Dué nez Guzmán, Alexander Sasha Vezhnevets, John P. Agapiou, Peter Sunehag, Raphael Koster, Jayd Matyas, Charles Beattie, Igor Mordatch, and Thore Graepel. Scalable evaluation of multi-agent reinforcement learning with melting pot. *PMLR*, 2021.

[17] J K Terry and Benjamin Black. Multiplayer support for the arcade learning environment. *arXiv preprint arXiv:2009.09341*, 2020.

[18] Xavier Puig, Tianmin Shu, Shuang Li, Zilin Wang, Yuan-Hong Liao, Joshua B Tenenbaum, Sanja Fidler, and Antonio Torralba. Watch-and-help: A challenge for social perception and human-ai collaboration. *arXiv preprint arXiv:2010.09890*, 2020.

[19] Ho Chit Siu, Jaime Peña, Edenna Chen, Yutai Zhou, Victor Lopez, Kyle Palko, Kimberlee Chang, and Ross Allen. Evaluation of human-ai teams for learned and rule-based agents in hanabi. *Advances in Neural Information Processing Systems*, 34:16183–16195, 2021.

[20] Christiane Attig, Patricia Wollstadt, Tim Schrills, Thomas Franke, and Christiane B Wiebel-Herboth. More than task performance: Developing new criteria for successful human-ai teaming using the cooperative card game hanabi. In *Extended Abstracts of the CHI Conference on Human Factors in Computing Systems*, pages 1–11, 2024.

[21] Nolan Bard, Jakob N Foerster, Sarath Chandar, Neil Burch, Marc Lanctot, H Francis Song, Emilio Parisotto, Vincent Dumoulin, Subhodeep Moitra, Edward Hughes, et al. The hanabi challenge: A new frontier for ai research. *Artificial Intelligence*, 280:103216, 2020.

[22] David E Rumelhart, Geoffrey E Hinton, Ronald J Williams, et al. Learning internal representations by error propagation, 1985.

[23] Kyunghyun Cho, Bart Van Merriënboer, Caglar Gulcehre, Dzmitry Bahdanau, Fethi Bougares, Holger Schwenk, and Yoshua Bengio. Learning phrase representations using rnn encoder-decoder for statistical machine translation. *arXiv preprint arXiv:1406.1078*, 2014.

[24] Cheng Chi, Zhenjia Xu, Siyuan Feng, Eric Cousineau, Yilun Du, Benjamin Burchfiel, Russ Tedrake, and Shuran Song. Diffusion policy: Visuomotor policy learning via action diffusion. *The International Journal of Robotics Research*, page 02783649241273668, 2023.

[25] Yuqi Wang, Jiawei He, Lue Fan, Hongxin Li, Yuntao Chen, and Zhaoxiang Zhang. Driving into the future: Multiview visual forecasting and planning with world model for autonomous driving. In *Proceedings of the IEEE/CVF Conference on Computer Vision and Pattern Recognition*, pages 14749–14759, 2024.

[26] Ye Yuan, Xinshuo Weng, Yanglan Ou, and Kris M. Kitani. Agentformer: Agent-aware transformers for socio-temporal multi-agent forecasting. In *Proceedings of the IEEE/CVF International Conference on Computer Vision (ICCV)*, pages 9813–9823, October 2021.

[27] Jingtao Ding, Yunke Zhang, Yu Shang, Yuheng Zhang, Zefang Zong, Jie Feng, Yuan Yuan, Hongyuan Su, Nian Li, Nicholas Sukiennik, et al. Understanding world or predicting future? a comprehensive survey of world models. *arXiv preprint arXiv:2411.14499*, 2024.

[28] Taisuke Kobayashis. q-vae for disentangled representation learning and latent dynamical systems. *IEEE Robotics and Automation Letters*, 5(4):5669–5676, 2020. doi: 10.1109/LRA.2020.3010206.

[29] Hang Zhao, Jiyang Gao, Tian Lan, Chen Sun, Ben Sapp, Balakrishnan Varadarajan, Yue Shen, Yi Shen, Yuning Chai, Cordelia Schmid, et al. Tnt: Target-driven trajectory prediction. In *Conference on Robot Learning*, pages 895–904. PMLR, 2021.

[30] Max Jaderberg, Valentin Dalibard, Simon Osindero, Wojciech M Czarnecki, Jeff Donahue, Ali Razavi, Oriol Vinyals, Tim Green, Iain Dunning, Karen Simonyan, et al. Population based training of neural networks. *arXiv preprint arXiv:1711.09846*, 2017.

[31] DJ Strouse, Kevin McKee, Matt Botvinick, Edward Hughes, and Richard Everett. Collaborating with humans without human data. *Advances in Neural Information Processing Systems*, 34:14502–14515, 2021.

[32] Xue Yan, Jiaxian Guo, Xingzhou Lou, Jun Wang, Haifeng Zhang, and Yali Du. An efficient end-to-end training approach for zero-shot human-ai coordination. *Advances in Neural Information Processing Systems*, 36:2636–2658, 2023.

[33] Yang Li, Shao Zhang, Jichen Sun, Yali Du, Ying Wen, Xinbing Wang, and Wei Pan. Cooperative open-ended learning framework for zero-shot coordination. In *International Conference on Machine Learning*, pages 20470–20484. PMLR, 2023.

[34] Chao Yu, Jiaxuan Gao, Weilin Liu, Botian Xu, Hao Tang, Jiaqi Yang, Yu Wang, and Yi Wu. Learning zero-shot cooperation with humans, assuming humans are biased. *arXiv preprint arXiv:2302.01605*, 2023.

[35] Rui Zhao, Jinming Song, Yufeng Yuan, Haifeng Hu, Yang Gao, Yi Wu, Zhongqian Sun, and Wei Yang. Maximum entropy population-based training for zero-shot human-ai coordination. In *Proceedings of the AAAI Conference on Artificial Intelligence*, volume 37, pages 6145–6153, 2023.

[36] Bidipta Sarkar, Andy Shih, and Dorsa Sadigh. Diverse conventions for human-AI collaboration. In *Thirty-seventh Conference on Neural Information Processing Systems*, 2023.

[37] Chao Yu, Akash Velu, Eugene Vinitsky, Jiaxuan Gao, Yu Wang, Alexandre Bayen, and Yi Wu. The surprising effectiveness of ppo in cooperative multi-agent games. *Advances in neural information processing systems*, 35:24611–24624, 2022.

[38] Ryan Lowe, Yi I Wu, Aviv Tamar, Jean Harb, OpenAI Pieter Abbeel, and Igor Mordatch. Multi-agent actor-critic for mixed cooperative-competitive environments. *Advances in neural information processing systems*, 30, 2017.

[39] Yancheng Liang, Daphne Chen, Abhishek Gupta, Simon Shaolei Du, and Natasha Jaques. Learning to cooperate with humans using generative agents. In *The Thirty-eighth Annual Conference on Neural Information Processing Systems*, 2024.

[40] Philipp Vollmuth, Martha Folty, Raymond Y Huang, Norbert Galldiks, Jens Petersen, Fabian Isensee, Martin J van den Bent, Frederik Barkhof, Ji Eun Park, Yae Won Park, et al. Artificial intelligence (ai)-based decision support improves reproducibility of tumor response assessment in neuro-oncology: An international multi-reader study. *Neuro-oncology*, 25(3):533–543, 2023.

[41] Paul Tylkin, Goran Radanovic, and David C Parkes. Learning robust helpful behaviors in two-player cooperative atari environments. In *Proceedings of the 20th international conference on autonomous agents and multiagent systems*, pages 1686–1688, 2021.

[42] Jijia Liu, Chao Yu, Jiaxuan Gao, Yuqing Xie, Qingmin Liao, Yi Wu, and Yu Wang. Llm-powered hierarchical language agent for real-time human-ai coordination. *arXiv preprint arXiv:2312.15224*, 2023.

[43] Kevin R McKee, Xuechunzi Bai, and Susan T Fiske. Warmth and competence in human-agent cooperation. *Autonomous Agents and Multi-Agent Systems*, 38(1):23, 2024.

[44] Guy Hoffman. Evaluating fluency in human–robot collaboration. *IEEE Transactions on Human-Machine Systems*, 49(3):209–218, 2019.

[45] Aurelie Beynier, Francois Charpillet, Daniel Szer, and Abdel-Illah Mouaddib. Dec-mdp/pomdp. *Markov Decision Processes in Artificial Intelligence*, pages 277–318, 2013.

[46] Craig Boutilier. Planning, learning and coordination in multiagent decision processes. In *TARK*, volume 96, pages 195–210. Citeseer, 1996.

[47] David Hsu, Tingting Jiang, John Reif, and Zheng Sun. The bridge test for sampling narrow passages with probabilistic roadmap planners. In *2003 IEEE international conference on robotics and automation (cat. no. 03CH37422)*, volume 3, pages 4420–4426. IEEE, 2003.

[48] Mitul Saha, Jean-Claude Latombe, Yu-Chi Chang, and Friedrich Prinz. Finding narrow passages with probabilistic roadmaps: The small-step retraction method. *Autonomous robots*, 19:301–319, 2005.

- [49] Jakub Szkandera, Ivana Kolingerová, and Martin Maňák. Narrow passage problem solution for motion planning. In *International Conference on Computational Science*, pages 459–470. Springer, 2020.
- [50] Sam Toyer, Rohin Shah, Andrew Critch, and Stuart Russell. The MAGICAL benchmark for robust imitation. In *Advances in Neural Information Processing Systems*, 2020.
- [51] Kevin Zakka, Andy Zeng, Pete Florence, Jonathan Tompson, Jeannette Bohg, and Debidatta Dwibedi. Xirl: Cross-embodiment inverse reinforcement learning. *Conference on Robot Learning (CoRL)*, 2021.
- [52] Matteo Bettini, Amanda Prorok, and Vincent Moens. Benchmarl: Benchmarking multi-agent reinforcement learning. *Journal of Machine Learning Research*, 25(217):1–10, 2024.

A Comparison with Other Environments

Environment	State/Action	Physics-based	Constraints	Collaboration Behaviors
Overcooked-AI	Discrete	No	Items placed only in specific locations	Passing items, dividing tasks, and collision avoidance
Table Carrying	Continuous	No	No physical feedback, task ends upon collision	Joint carrying (i.e., action consistency)
Moving Out	Continuous	Yes	Realistic physics, friction, collision feedback, diverse items with physical properties.	Coordination, Awareness of needing help, joint carrying (i.e., action consistency).

Metrics	Pros	Cons	Human Data
Number of cooked onions in a limited time	Small state/action space, fast training, human data available	Limited behavior variety, simple tasks	Yes
Success rate, Completion time	Continuous actions	No physics in interactions, single task, no dataset	No
Task Completion Rate, Normalized Final Distance, Waiting Time, Action Consistency	Realistic physics, multiple collaboration modes, physics feedback, human dataset available	Higher computational cost	Yes

Table 2: Comparison between Moving Out, Overcooked-AI, and Table Carrying. Overall, Moving Out offers more diverse collaboration modes and physical constraints due to its physics-based environment.

B Comparison with Oracle Simulation

	NFD↑		Prediction Accuracy	
	Task 1	Task 2	Task 1	Task 2
DP + BASS	0.5733	0.5535	0.6250	0.4870
DP + BASS w/Oracle Simulator	0.5875	0.6209	N/A	N/A

Table 3: Performance of different simulation strategies. The oracle simulator serves as the upper bound for our method.

We compare the task completion (NFD) and prediction accuracy of actions against the oracle simulator (i.e., the 2D physics engine) in Table 3. We compute the prediction accuracy by comparing the actions selected using our next state predictor versus the actions selected using the oracle simulator. The oracle simulator serves as the upper bound for our action selection method since it provides the ground-truth next states. We observe that our model achieves higher accuracy in Task 1, with results that are closer to those of the oracle simulator. This is because Task 1 uses a fixed map, while Task 2 trains on randomized states.

C MAPPO Training Setting

To train MAPPO, we integrate the Moving Out environment into the BenchMARL [52] multi-agent RL library. Our approach to MAPPO training was designed to align with the objectives of Task 1 and Task 2, which were initially conceptualized with dataset-driven methods in mind. We adapted the conditions for MAPPO as follows:

For Task 1, which originally involved training on data collected from some human players and testing on data from unseen human players, we interpret this as a zero-shot coordination challenge for MAPPO. This setup evaluates their ability to develop coordination strategies from scratch in the absence of direct human examples.

For Task 2, the initial idea was to train on maps with diverse physical characteristics and then evaluate generalization to environments with unseen physical features. To mirror this for MAPPO, the agents are trained on maps where various physical properties (object masses, shapes, and sizes) are randomized, similar to the randomization process used during data collection for behavior cloning. Following this training phase, MAPPO’s performance is then evaluated on maps with fixed physical characteristics that were not encountered during training.

C.1 Hyperparameters

Table 4: Summary of Parameters for MAPPO

Parameter Name	Value
Share Policy Parameters	True
Share Policy Critic	True
Gamma (γ)	0.99
Learning Rate	0.00005
Adam Epsilon	0.000001
Clip Gradient Norm	True
Clip Gradient Value	5
Soft Target Update	True
Polyak Tau (τ)	0.005
Hard Target Update Frequency	5
Initial Exploration Epsilon	0.8
Final Exploration Epsilon	0.01
Clip Epsilon	0.2
Critic Coefficient	1.0
Critic Loss Type	12
Entropy Coefficient	0
Lambda (λ) for GAE	0.9
Max Cycles Per Episode	1000
Max Frames	30,000,000
On-Policy Collected Frames Per Batch	6000
On-Policy Environments Per Worker	10
On-Policy Minibatch Iterations	45
On-Policy Minibatch Size	400
Model Type	MLP
Linear Layer Sizes	[256, 256]
Activation Function	<code>torch.nn.Tanh</code>

For coordination maps, due to the greater distance from the initial explorer positions to the target items and the presence of more walls, we increased `max_cycles_per_episode` from 1000 to 3000. Concurrently, we adjusted `entropy_coef` to 0.00065 and `gamma` to 0.92 for these maps.

D Reward Setting

D.1 Dense Reward Setting

The dense reward is based on the change in distance $\Delta d = d_{\text{prev}} - d_{\text{curr}}$, scaled by a factor $\gamma = 20$, where d_{prev} and d_{curr} denote the agent's distance to the current target at the previous and current timestep, respectively. When the agent is not holding an object, the target is either the nearest unheld item or a middle/large item currently being moved by another agent that requires assistance. When the agent is holding an object, the target becomes the goal region. At each timestep, the agent receives a reward of $\Delta d \times \gamma$. See Tab. 5 for more details.

Additionally, there are special rewards tailored for specific maps. In Map 11 (Four Corners), for instance, two agents need to hold the two short sides of a rectangular item to more easily pass through a path successfully. Therefore, to encourage this, the reward calculation for the agents' distance to this item has been modified: instead of being based on the distance to the item's center point, it is now calculated based on the distance to its two short ends. This change is designed to encourage the agents to grasp the rectangle by its short ends.

Table 5: Dense Reward Settings

Primary State / Event	Specific Condition	Reward Value
<i>A. Distance-based Rewards</i>		
Agent not holding an item	Agent moves closer to the nearest available item	$\Delta d \times \gamma$
	Agent moves closer to a middle or large item currently held by another agent	$\Delta d \times \gamma$
Agent holding an item	Agent moves closer to the nearest goal region	$\Delta d \times \gamma$
<i>B. Event-based Rewards: Agent Holds an Item</i>		
Agent successfully holds an item	Default reward for picking up	+0.5
	<i>Exception:</i> If another agent is already holding other middle or large item at this time	-0.5 (total for this hold event)
	<i>Exception:</i> If the item picked up was already located within a goal region	-0.5 (total for this hold event)
<i>C. Event-based Rewards: Agent Unholds an Item</i>		
Agent successfully unholds an item	Item is released inside a goal region	+0.5
	Item is released <i>not</i> inside a goal region	-0.5
	<i>Exception:</i> If another agent needs help, holding a large or middle item outside the goal region, at the moment of unholding.	+0.5 (additive)
<i>D. Time-based Reward (Step Cost)</i>		
Each timestep	Agent exists in the environment	-0.01

D.2 Does MAPPO work in Moving Out with sparse reward setting?

The primary challenge in Moving Out lies in its significantly larger and more complex state space. Within such an expansive environment, agents who take random exploration struggle to successfully complete the multi-step tasks required to reach goal states and thus rarely receive the sparse or event-based rewards crucial for learning. Consequently, sparse reward formulations currently appear insufficient for effective policy learning in Moving Out.

MAPPO algorithms employing sparse or event-based rewards have achieved notable success in environments such as Overcooked-AI. This success can be largely attributed to the characteristics of Overcooked-AI, specifically its discrete action-state space and relatively compact overall state space. These features allow agents to encounter rewarding events with sufficient frequency through exploration, even when rewards are not dense, facilitating effective policy learning.

In Overcooked, the state-action space is small and discrete, with only tens of possible states and six possible actions, effectively rendering it a tabular setting. In contrast, our environment features continuous state and action spaces, states include precise map coordinates, and actions involve continuous control over speed and direction. Although RL is relatively easy for small discrete space, extending methods to handle continuous space is non-trivial.

Moreover, the tasks in Overcooked are relatively simple: agents fetch onions from a fixed area and deliver them using plates. Onions and plates are homogeneous, unlimited, and confined to designated regions. Once picked up, items can only be placed in predefined locations for handoff, simplifying coordination between agents.

By comparison, our tasks are significantly more complex with additional physical constraints. First, the items in our environment are heterogeneous, which are randomized in shape, size, and initial position. Thus, agents must learn to generalize over combinations of all possible scenarios. Second, unlike Overcooked, where items can only be placed in fixed zones, our agents can place items anywhere on the map. This greatly increases the difficulty of learning how to transfer items to target locations or hand them off between agents, especially in a continuous space. Additionally, our framework requires agents to engage in a wider range of collaborative behaviors beyond simple item passing—for instance, jointly moving large objects or coordinating to rotate items in tight spaces like wall corners. This diversity of collaboration types introduces further complexity.

E Comparative analysis of the Behaviors of BC and RL agents

The fundamental difference between Behavior Cloning (BC) and MAPPO lies in their learning mechanisms and resulting agent behaviors. BC methods are inherently data-driven, leading to policies whose actions and overall effectiveness closely mirror the human behaviors captured in the training dataset. In contrast, MAPPO, as a reinforcement learning (RL) approach, develops behaviors that are strongly guided by the specific design of its dense reward function.

This distinction is evident in specific scenarios. For instance, on Map 6 (Distance Priority), both agents have their closest middle-sized items. However, human demonstration data frequently shows a strategy of first securing two smaller items before returning to move a middle-sized item together. A MAPPO agent, guided by a dense reward that incentivizes moving the nearest object, will typically prioritize the closer middle-sized item. If two such items are equidistant to respective agents (e.g., a pink agent targeting a yellow star and a blue agent targeting a blue circle), the initial actions will be independent. The coordination emerges when one agent successfully grasps a middle-sized item; the reward structure then incentivizes the other agent to assist with that specific item. Thus, the RL behavior can appear as a race to secure a primary middle-sized object, with the "loser" then being redirected by rewards to help the "winner." BC models on Map 6 (Distance Priority), however, reflect the diversity of the human dataset. This dataset contains instances of both "small-items-first" and "middle-item-first" strategies. Consequently, a BC agent might exhibit behaviors where one agent targets a middle-sized item while the other simultaneously attempts to move a small item, reflecting a momentary misalignment as different agents emulate distinct strategies observed in the human data.

Map 11 (Four Corners) further illustrates these differences. Here, two agents might each have two items at an equal distance, making multiple initial moves potentially optimal. In our MAPPO training, agents often exhibit initial movements that appear somewhat exploratory or randomized until one agent commits to and grasps a large item. At this point, the dense reward system effectively directs the other agent to provide assistance. Conversely, BC models on Map 11 (Four Corners) tend to display more decisive and rapidly aligned behavior from the start. Observations of the human dataset for this map revealed a common leader-follower dynamic, where one player (e.g., the blue agent) consistently follows the lead of the other (e.g., the pink agent). If the pink agent, for example, decisively moves towards an upper pink square, the blue agent often follows suit immediately to assist. As a result, BC models rarely exhibit prolonged periods of uncoordinated or hesitant movement before aligning on a common goal.

In summary, BC methods excel at reproducing observed human behaviors, including their specific strategies and inherent diversity. RL approaches like MAPPO, while capable of discovering effective strategies, are highly sensitive to the nuances of reward function design. Even slight modifications to the reward signals can lead to significant and sometimes qualitatively different emergent behaviors in the trained agents.

F Details of Evaluation Metrics

We assess human-AI collaboration in Moving Out using the following metrics.

Task Completion Rate (TCR) The proportion of items successfully moved to the goal regions, weighted by size:

$$TCR = \frac{\sum w_i \mathbb{I}(o_i \text{ delivered})}{\sum w_i}$$

where $w_i = 1$ (small) or 2 (middle/large). Range: $[0,1]$.

Normalized Final Distance (NFD) The distance between objects and the closest goal regions, recognizing partial progress as valuable.

$$NFD = 1 - \frac{\sum_{i=1}^N d_i^{\text{final}}}{\sum_{i=1}^N d_i^{\text{initial}}},$$

where d_i^{initial} and d_i^{final} are the object's initial and final distances to the target.

Waiting Time (WT) The total time an agent waits for help.

$$WT = \sum_{t \in \mathcal{W}} (t_{\text{end}}^t - t_{\text{start}}^t),$$

where \mathcal{W} is the set of time intervals when an agent holds a middle or large object but waits for help. t_{start}^t and t_{end}^t mark the waiting period.

Action Consistency (AC) This metric quantifies how well two agents align their forces when moving a middle or large object, indicating coordination efficiency.

$$AC = \frac{1}{T} \sum_{t=0}^{T-1} \frac{\|(\vec{f}_1^t + \vec{f}_2^t) \cdot \vec{d}_t\|}{\|\vec{f}_1^t\| + \|\vec{f}_2^t\|},$$

where \vec{f}_1^t, \vec{f}_2^t are the forces applied by the agents at time t , \vec{d}_t is the unit vector connecting their positions, and T is the total timesteps. The value ranges from 0 to 1, with 1 indicating perfect alignment.

G Implementation Details

G.1 Environment Details

G.1.1 Observation Encoding

State Observation Our observation encoding is ego-centric and represents all information as a one-dimensional vector. The encoded information includes:

- Self: Position and angle, with angles θ represented using $[\cos \theta, \sin \theta]$. A boolean value indicates whether the agent is holding an item (True/False).
- Partner: Position, angle, and whether it is holding.
- Items: Each item is encoded with position, angle, size, category, and shape. Category and shape use a one-hot encoding.

When training on a single map, the walls and goal region remain unchanged, so we do not encode them. However, when training across different maps, we include their encoding:

- Walls: Represented by the (x, y) coordinates of the top-left and bottom-right corners.
- Goal Region: Represented the same as walls. The top-left and bottom-right corners.

G.1.2 Action Encoding

The agent's action space has four values:

- The movement distance (forward or backward).
- The target angle (encoded using cos and sin).
- The grasping action: 1 means grasp or release, 0 means no change.

G.2 Baseline Details

- **Diffusion Policy**: We follow the original implementation by [24] for the model architecture, which employs a 1D U-Net to generate action sequences. The observation, prediction, and executable horizons are set to 2, 8, and 4, respectively. Training is performed using the Adam optimizer with 1k epochs, 1024 batch size, and 0.001 learning rate. The diffusion steps are 36. The grasp action is encoded by one-hot encoding.
- **MLP** The MLP model consists of 3 fully connected layers with Tanh activation and hidden_dim 2048. It concatenates one past state and one current state as input and predicts actions for the next 8 steps. Training is performed using the Adam optimizer with 1k epochs, 1024 batch size, and 0.001 learning rate. It optimizes a combination of mean squared error (MSE) loss for movement outputs and cross-entropy loss for grasp action predictions.
- **GRU** uses a GRU layer followed by 3 fully connected layers with Tanh activation and hidden_dim 2048. It takes one past state and the current state as input and predicts actions for the next 4 steps. The model processes sequential data and learns action patterns based on previous movements. Training is performed using the Adam optimizer with 1k epochs, 1024 batch size, and 0.001 learning rate. It optimizes a combination of mean squared error (MSE) loss for movement outputs and cross-entropy loss for grasp action predictions.

G.3 BASS Details

- **Dynamics Model** The Autoencoder consists of an encoder and a decoder, both made of two linear layers. They use ReLU as the activation function, and each layer has 128 units. The latent space has 32 dimensions. The dynamics Model is a two-layer MLP (Multi-Layer Perceptron). Each hidden layer has 128 units. During training, the two autoencoders and the dynamic model are trained together. Additionally, we also explored fine-tuning the second AE from the first. Our ablation on selected Maps 2, 6, & 9 shows the following average NFDs: 1) Joint training: 0.55, 2) Fine-tuning the second AE from the first AE: 0.50, 3) Training two AEs separately: 0.48.
- **Partner Action Predictor** The Partner Action Predictor can be designed based on the application. In some cases, it can be the same as the action policy, but with a small change: it swaps the agent's state with the partner's state. This allows the model to predict the partner's action from their perspective.

Behavior Augmentation and Recombination Sub-Trajectories In behavior augmentation, we add noise with a mean of 0 and a standard deviation of 0.002. In recombination sub-trajectories, since two points in a continuous space are almost never the same, we set a tolerance value. We discretize the environment into a 48×48 grid. If the robot's start and end points are in the same grid cell, we treat them as the same point.

Normalized Final Distance Calculation Many maps have walls, so we cannot use Euclidean distance. To improve efficiency, we discretize the environment into a 48×48 grid. We use the BFS algorithm to compute the distance from the item to the Goal Region.

Can BASS be used as a standalone Method beyond Moving Out? BASS is a standalone method composed of two components. Together, they make BASS applicable across various behavior cloning methods outside of Moving Out, as discussed. We tested BASS on a widely used human-AI collaboration environment, Overcooked AI, specifically, the "Cramped Room" map. The results showed that DP+BASS improved the score by 15% compared to DP alone. This demonstrates that BASS is not limited to Moving Out.

H Data Collection: Training Data

We conducted data collection for two tasks, each designed to evaluate different aspects of human-AI collaboration. For the two tasks, each participant controlled an agent using a joystick. The environment running at 10Hz for data collection.

For **Task 1**, which focuses on human behavior diversity, we recruited 36 participants, forming 18 groups of two. Before data collection, each group underwent a 10-minute practice session to familiarize itself with the environment. The remaining 50 minutes were dedicated to data collection. Each pair played each map three times, then switched agents and played three more times, resulting in six demonstrations per map. If a group completed all maps, they contributed a total of $12 \times 6 = 72$ human demonstrations. However, not all groups completed the full set, with some collecting only 3 to 5 demonstrations per map. Additionally, we removed low-quality demonstrations where performance was significantly poor. In total, we collected 1,000 valid human demonstrations for this task.

For **Task 2**, which evaluates adaptation to physical constraints, we worked with four expert players who were highly familiar with the environment. Each map had randomized object properties, ensuring variation in shape, size, and mass. Each map was played 60 times, resulting in $60 \times 12 = 720$ human demonstrations.

Our data collection and human study process was approved by the Institutional Review Board (IRB) at the University of Virginia (UVA), under protocol IRB-SBS #6932. Participants were compensated based on the amount of data they contributed, receiving between \$15 to \$20 per hour.

I Computing Resources

I.1 Training

I.1.1 Behavior Cloning

Models MLP and GRU are trained for 1000 epochs within approximately 0.5 to 1 hour on a single A6000 GPU. Training a diffusion policy, while also for 1000 epochs, generally requires a longer period of 1 to 3 hours. Overall, the computational time for behavior cloning methods is comparatively short.

I.1.2 MAPPO

As MAPPO learns through direct interaction with the environment, it inherently requires a significantly greater number of training iterations. Currently, training MAPPO with 15 CPU threads typically spans 5 to 15 hours. Although MAPPO utilizes a lightweight MLP model with a small number of parameters, its training duration is extended due to two main factors:

- Firstly, the simulation environment, which is based on Pymunk, does not support GPU acceleration, thereby limiting the speed of physics calculations and environment stepping.
- Secondly, the computation of distance-based rewards becomes a bottleneck, particularly in environments featuring complex wall structures that necessitate more intensive calculations.

I.2 Inference Speed of DP/BASS

Inference speed is critical for real-time human-AI collaboration, especially when interacting with human partners. In our setup, the environment runs at 10 Hz, i.e., each step occurs every 100 ms. While diffusion models are generally slower, our implementation generates the next 8 actions in 69 ms on an NVIDIA RTX A6000 GPU. This allows us to interact in real-time by predicting one step in advance – at time step t , the agent executes the action predicted at $t-1$. This ensures smooth interaction without perceivable lags.

J Human Study: Playing with Models

J.1 Human Study Procedure

To collect data for our project, we designed an interactive experiment where human volunteers collaboratively played with trained AI agents. The data collection process is detailed as follows:

- **Model Selection:** Each volunteer was asked to select a model ID from four provided models (A, B, C, D).
- **Task Description and Limits:** After selecting a model, the volunteer played collaboratively with the AI agent across all twelve maps sequentially. The objective was to move all items on the map into the designated goal region. Each map had a time limit of 50 seconds. The volunteer could proceed to the next map either by successfully moving all items into the goal region or upon reaching the 50-second time limit.
- **Agent Roles:** For the first two models (A and B), the volunteer controlled the "red" agent while the AI controlled the "blue" agent. For the remaining two models (C and D), the roles were switched, with the volunteer controlling the "blue" agent and the AI taking the role of the "red" agent.
- **Questionnaire:** After completing all 12 maps for a given model, the volunteer filled out a questionnaire consisting of eight Likert-scale questions and one free-response question. Responses on the Likert scale ranged from "strongly agree" to "strongly disagree."

In total, we conducted this experiment with 12 volunteers. Each volunteer will be paid \$20 for one hour of playing.

J.2 Questionnaire

We use the 7-Point Likert Scale for the questions below:

1. **Teamwork:** The other agent and I worked together towards a goal.
2. **Humanlike:** The other agent's actions were human-like.
3. **Reasonable:** The other agent always made reasonable actions throughout the game.
4. **Follow:** The other agent followed my lead when making decisions.
5. **Physics:** The other agent understands how to work with me when objects have varying physical characteristics.
6. **Helpfulness:** The other agent understands my intention and proactively helps me when I need assistance.
7. **Collision:** When our movement paths conflict, the other agent and I can effectively coordinate to avoid collisions.
8. **Alignment:** When moving large items together, our target directions remain well-aligned.
9. **Future:** I would like to collaborate with the other agent in future Moving Out tasks.

K Results of Different Methods with BASS

Task 1	Methods	TCR↑		NFD↑		WT ↓		AC↑	
		Mean	Std Error						
MLP		0.3568	0.0508	0.4118	0.0338	0.4380	0.0419	0.7890	0.0250
+ BASS w/o Simulation		0.2952	0.0436	0.4207	0.0359	0.3639	0.0358	0.8060	0.0126
GRU		0.3070	0.0479	0.3674	0.0365	0.3143	0.0532	0.7618	0.0201
+ BASS w/o Simulation		0.4117	0.0465	0.4396	0.0350	0.3891	0.0418	0.8225	0.0173
+ BASS w/o Augmentation		0.3531	0.0411	0.4047	0.0373	0.3835	0.0419	0.8195	0.0210
+ Full BASS		0.4120	0.0513	0.4454	0.0392	0.4218	0.0426	0.8345	0.0173
Diffusion Policy (DP)		0.3829	0.0681	0.4818	0.0514	0.3075	0.0374	0.8395	0.0216
+ BAAS w/o Simulation		0.4028	0.0666	0.5114	0.0493	0.3392	0.0428	0.8242	0.0254
+ BASS w/o Augmentation		0.4741	0.0667	0.5561	0.0506	0.3176	0.0435	0.8495	0.0174
+ Full BASS		0.5027	0.0619	0.5707	0.0468	0.3448	0.0402	0.8615	0.0167

Table 6: The table presents all experimental results for Task 1

Task 2	Methods	TCR↑		NFD↑		WT ↓		AC↑	
		Mean	Std Error						
MLP		0.2557	0.0413	0.3602	0.0315	0.4867	0.0418	0.8175	0.0261
+ BASS w/o Simulation		0.2014	0.0336	0.3656	0.0244	0.3657	0.0332	0.7890	0.0250
GRU		0.2582	0.0509	0.3935	0.0428	0.4680	0.0594	0.8487	0.0183
+ BASS w/o Simulation		0.3333	0.0539	0.4141	0.0439	0.5611	0.0587	0.8513	0.0286
+ BASS w/o Augmentation		0.3670	0.0522	0.4246	0.0420	0.4365	0.0593	0.8572	0.0222
+ Full BASS		0.3414	0.0522	0.4410	0.0442	0.4379	0.0596	0.8754	0.0165
Diffusion Policy (DP)		0.3125	0.0564	0.4526	0.0427	0.3100	0.0385	0.8442	0.0184
+ BAAS w/o Simulation		0.3569	0.0547	0.4908	0.0385	0.3256	0.0431	0.8373	0.0147
+ BASS w/o Augmentation		0.4200	0.0544	0.5187	0.0417	0.3232	0.0417	0.8305	0.0169
+ Full BASS		0.4348	0.0599	0.5535	0.0423	0.3096	0.0451	0.8474	0.0128

Table 7: The table presents all experimental results for Task 2

L Map Analysis

L.1 Coordination

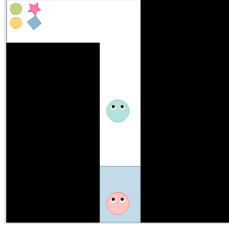
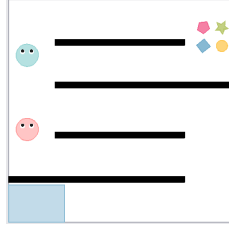
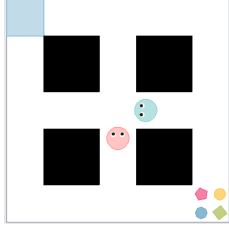
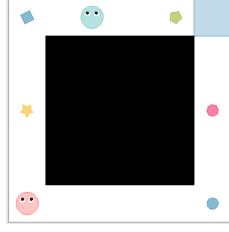
Map	Analysis	Map	Analysis
	<p><i>Map 1: Hand Off</i> is designed with a single narrow pathway that forces the agent, the one that is closer to the items, to efficiently pass them to the other agent.</p>		<p><i>Map 2: Pass Or Split</i> features four non-intersecting pathways, designed to evaluate the agents' ability to select the most suitable path while considering the need for collaboration.</p>
	<p><i>Map 3: Efficient Routes</i> features several pathways leading to the goal region, allowing the agents to independently determine the most efficient path while considering the movement of the other agent.</p>		<p><i>Map 4: Priority Pick</i> creates an environment that requires each agent to independently decide whether to prioritize moving the item closer to the goal region first or bringing the farther item closer.</p>

Table 8: Maps categorized under **Coordination**.

L.2 Awareness

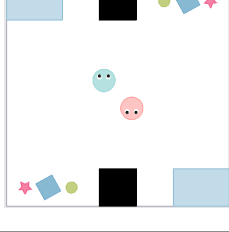
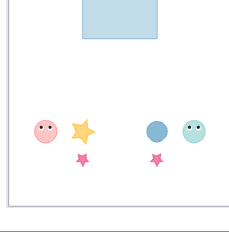
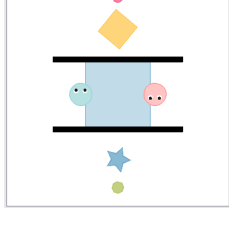
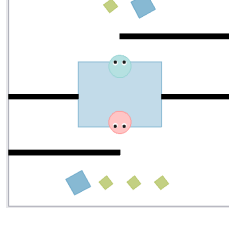
Map	Analysis	Map	Analysis
	<p><i>Map 5: Corner Decision</i> requires the agents to decide whether to follow the other agent to the upper right or the lower left corner and to determine which size of item to prioritize moving first.</p>		<p><i>Map 6: Distance Priority</i> contains two medium-sized items, requiring the agents to decide whether to prioritize the item that is farther away or the one that is closer.</p>
	<p><i>Map 7: Top Bottom Priority</i> contains two items, either large or medium-sized, requiring the agents to decide whether to prioritize the item at the top or the one at the bottom.</p>		<p><i>Map 8: Adaptive Assist</i> contains a mix of large or medium-sized items and small items, requiring the agents to decide whether to prioritize collaborating on the larger item or individually handling the smaller item.</p>

Table 9: Maps categorized under **Awareness**.

L.3 Action Consistency

Map	Analysis	Map	Analysis
	<p><i>Map 9: Left Right</i> contains large-sized items, requiring the agents to continuously collaborate and make strategic decisions about whether to move items to the left or right goal region.</p>		<p><i>Map 10: Single Rotation</i> contains one large-sized item, which is designed to evaluate how well the two agents can collaborate to perform a single rotation.</p>
	<p><i>Map 11: Four Corners</i> contains large-sized items positioned at the four corners, requiring the agents to continuously collaborate by moving the items in either a clockwise or counter-clockwise order.</p>		<p><i>Map 12: Sequential Rotations</i> contains one large-sized item, which is designed to evaluate how well the two agents can collaborate to maintain a sequence of rotations.</p>

Table 10: Maps categorized under **Action Consistency**.